Self-Reinforcing Cascades: A Spreading Model for Beliefs or Products of Varying Intensity or Quality

Laurent Hébert-Dufresne [1,2,3] Juniper Lovato [1,2] Giulio Burgio [1] James P. Gleeson [4]
S. Redner [3,1] and P. L. Krapivsky [5,3]

[1]*Vermont Complex Systems Institute, University of Vermont, Burlington, Vermont, USA*
[2]*Department of Computer Science, University of Vermont, Burlington, Vermont, USA*
[3]*Santa Fe Institute, 1399 Hyde Park Road, Santa Fe, New Mexico 87501, USA*
[4]*MACSI, Department of Mathematics and Statistics, University of Limerick, Limerick, Ireland*
[5]*Department of Physics, Boston University, Boston, Massachusetts 02215, USA*

Models of how things spread often assume that transmission mechanisms are fixed over time. However, social contagions—the spread of ideas, beliefs, innovations—can lose or gain in momentum as they spread: ideas can get reinforced, beliefs strengthened, products refined. We study the impacts of such self-reinforcement mechanisms in cascade dynamics. We use different mathematical modeling techniques to capture the recursive, yet changing nature of the process. We find a critical regime with a range of power-law cascade size distributions with nonuniversal scaling exponents. This regime clashes with classic models, where criticality requires fine-tuning at a precise critical point. Self-reinforced cascades produce critical-like behavior over a wide range of parameters, which may help explain the ubiquity of power-law distributions in empirical social data.

Introduction—Cascades of beliefs, ideas, or news often show signs of criticality despite coming from various sources and spreading through different mechanisms [1]. The signature of criticality is a power-law tail in the cascade size distribution, scaling as $s^{-\tau}$. Cascade models predict this behavior at a precise critical point, the phase transition between a regime where all cascades eventually go extinct and another where they can grow infinitely. At this point, cascade models that follow a branching process structure universally predict a scaling exponent of $\tau = 3/2$ [2]. We call this critical exponent universal because, for a large family of spreading mechanisms, its value does not depend on the details of the model [3]. However, social media data show that cascade sizes can follow power-law distributions with scaling exponents much different from the prediction $\tau = 3/2$. The size of message cascades and reply trees appear to decay much faster with scaling exponents of $\tau = 3.9$ [4] and 4 [5], as do reposting cascades or recruitment to social movements both with exponents $\tau = 2.3$ [6,7], and many other data sources on platforms with exponents around $\tau = 2$ [1]. The difference between the universality

observed in models and the diversity of empirical results is yet unexplained.

Although cascade models vary, the vast majority of them use fixed mechanisms such that the same rules apply at every step of the cascade. For example, a new case of a disease produces infections through the same mechanism as previous cases. However, cascades of beliefs and ideas might be different. Beliefs can be self-reinforced [8] or modulated by social interactions [9]. Ideas or products can be refined as they are transmitted from one person to another.

Self-reinforcing cascade (SRC) model—Imagine a cascading product like a meme, conspiracy theory, rumor, or a piece of software spreading in a population of agents. At every transmission step in the cascade, the product has the chance to independently improve with probability p or get worse with probability $1 - p$. This process can stop for two reasons: either the quality of the product drops to zero, or the agents sharing it cannot find others to pass it on to (see Fig. 1).

As an example, consider open source projects where a seed piece of software is made available for others to fork and modify [10]. These modifications can either enhance or degrade the software, as well as its governance [11,12]. For instance, better code or governance might make the software more accessible and easier to adopt and update, while poorly written code or bad governance practices can make the software difficult to maintain, eventually leading to its abandonment [13]. As a result, the quality of the
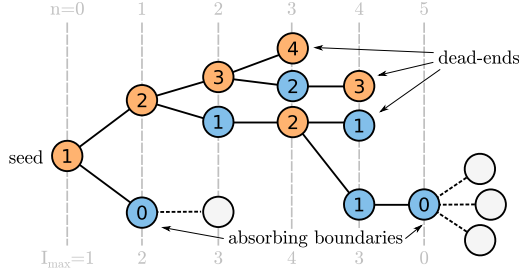
FIG. 1. Schematic of a self-reinforcing cascade. Start with a seed of intensity one. At each generation n, the process gains a unit of intensity when reaching active neighbors (orange); or, loses a unit of intensity when reaching inactive neighbors (blue). Paths of the cascade end when they reach a node with no children (dead end) or when the intensity falls to zero (absorbing boundary). The final cascade consists of all nodes where the process had positive intensity.
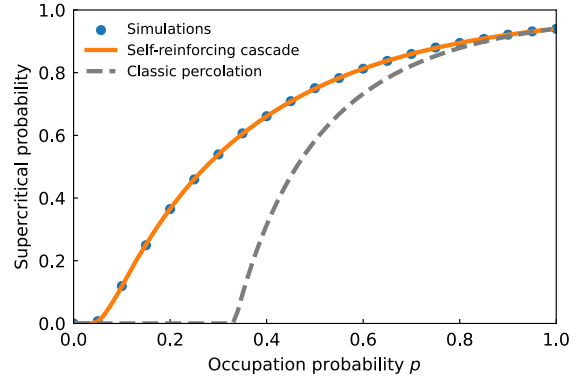

FIG. 2. Phase transitions of SRC and directed percolation on Poisson trees of average branching number $\ell = 3$. For the SRC, we compare our recursive exact solution based on Eq. (1) to simulations. The critical point marking the emergence of a supercritical cascade is at $p = 1/\ell = 1/3$ for percolation and at $p = (1 - 2\sqrt{2}/3)/2 \approx 0.0286$, as computed from Eq. (4), for the SRC.

software varies with each iteration, demonstrating the dynamic nature of such cascades.

As a final and very different example, we note that we originally conceived the self-reinforcing mechanism as a model of forest fires gaining intensity as they burn trees but losing intensity as they traverse gaps in forest cover [14]. We explore this idea that cascades can deviate from universal classes when they can be amplified or attenuated as they spread.

The SRC model shares conceptual similarities with other models accounting for popularity-driven nature of many cascades, using self-exciting point processes [15] or competition between cascades [16]. Cascade models based on these mechanisms can help explain two different universality classes, $\tau = 3/2$ and $\tau = 2$ [15], and interpolate between [16].

More generally, the SRC model provides a cascade perspective on killed branching random walks where certain results are known for its critical point in a continuous limit [17] and bounds on its critical behavior in the discrete case [18]. Here, we provide exact recursive solutions, static closed-form expressions for the expected cascade sizes and their critical point, and a dynamic analysis of cascade intensity. Beyond theoretical contributions, our results illustrate how diverse scaling exponents can easily be observed in cascades and we provide estimates for the exponents produced by the SRC model.

Recursive solution—Mathematically, we consider a general branching structure for contacts within the population. At any node, we define $G(x) = \sum_b \pi_b x^b$ as the probability generating function (PGF) for the number of "children" neighbors (occupied or not) of that node, π_b being the probability of branching into exactly b children [19]. The probability π_0 is equal to the probability that any node in the cascade is a dead end without children, one of two ways for a chain of transmission to end. Importantly, and in line with recent empirical findings [20], the branching number b

is drawn independently and identically at each node. However, intensity-dependent distributions for the branching number are a straightforward extension of the model (explored in Supplemental Material).

We pick the first node on this structure to start a cascade of intensity 1 (more generally, I_0). Any potential children will be either receptive to the process with probability p, and continue the process with intensity 2; or nonreceptive, such that they end their branch of the cascade by reaching intensity 0. In the next step, children with nonzero intensity in the last step (if any) can recruit their own receptive children (if any) to continue the process with intensity 3; or convince their nonreceptive children (if any) to continue the process with intensity 1. In general, intensity increases when the cascade spreads to receptive nodes and decreases when it spreads to nonreceptive ones. Any branch of the cascade dies either when it reaches a dead end or when its intensity goes to zero.

We can solve this process using a self-consistent recursive solution. Let $H_1(x)$ be the PGF for the cascade size distribution of a node of intensity 1 [21]. Since the root node is part of the cascade, $H_1(x)$ has to be proportional to x to count that node. After that, every possible child generated by $G(x)$ is either receptive with probability p or nonreceptive otherwise. Receptive children will have intensity 2 and produce cascades whose size is generated by $H_2(x)$, while nonreceptive children will have intensity 0 and thus lead to trivial cascades of size 0, i.e, $H_0(x) = x^0 = 1$. We can therefore write $H_1(x) = xG[pH_2(x) + (1 - p)]$ to define a recursive self-consistent equation for the cascade size distribution. In this equation, we use the fact that a cascade produced by a node is the sum of the cascades produced by its children, and that the PGF for the sum of a variable number of independent random variables is the composition of the PGFs.

More generally, we can write

$$H_k(x) = xG[pH_{k+1}(x) + (1-p)H_{k-1}(x)] \quad (1)$$

as nonreceptive nodes decrease the intensity but do not necessarily end the process if $k > 1$. To close the second-order recursion in Eq. (1) we need another boundary condition besides $H_0(x) = 1$. To this end, we define $\bar{k}$ as the maximum intensity allowed, implemented by requiring $H_{\bar{k}+1}(x) = H_{\bar{k}}(x)$.

All closed-form solutions presented below hold in the limit $\bar{k} \to \infty$, i.e., for cascades with no upper bound on intensity. All numerical simulations are performed in this limit. In practice, integrating Eq. (1) requires choosing a finite $\bar{k}$. However, as shown in the following, cascades seeded at an intensity enough smaller than $\bar{k}$ are insensitive to the latter, which is thus effectively indistinguishable from $\bar{k} \to \infty$.

To solve Eq. (1), we iterate it for multiple values of x, up to $\bar{k} = 100$, until all values converge to within a certain precision threshold (we use 10^{-12}). Once a fixed point has been reached, we can extract $H_1(x)$, which generates the cascade size distribution from the seed (assuming $I_0 = 1$). We can also obtain the probability that a cascade is supercritical and never ends as $1 - H_1(1)$, since infinite cascades are not accounted for in Eq. (1). Methods are detailed in our Supplemental Material (SM) [22] and our calculations are available online [23].

Critical point—We first look at the phase transition of SRC in Fig. 2. We assume that the number of children nodes is drawn from a Poisson distribution $\pi_b = \ell^b e^{-\ell}/b!$ of mean $\ell \geq 1$. The self-intensifying mechanism greatly reduces the critical point of the process. For an average branching number $\ell = 3$, we find p_c at $(1 - 2\sqrt{2}/3)/2 \approx 0.0286$ instead of $1/\ell = 1/3$ for the emergence of a giant connected component (infinite-size) cascade in a random network [24].

We now derive a closed-form solution for the critical point. To gain some insights into the expected behavior of Eq. (1), we rewrite the system as a recursion over the expected cascade size $m_k(p)$ when starting at a node of intensity k for a given p. To calculate $m_k(p)$, we average the cascade size distribution by taking the derivative of $H_k(x)$ and evaluating at $x = 1$ (with $H_k(1) = 1$ in the subcritical regime), to obtain

$$m_k(p) = 1 + \ell p m_{k+1}(p) + \ell(1-p)m_{k-1}(p). \quad (2)$$

This is a second-order linear difference equation with boundary conditions $m_1(p) = 1 + \ell p m_2(p)$ and $m_{\bar{k}}(p) = 1 + \ell p m_{\bar{k}}(p) + \ell(1-p)m_{\bar{k}-1}(p)$. In the limit of large $\bar{k}$, we obtain the exact solution (see SM for derivation [22])
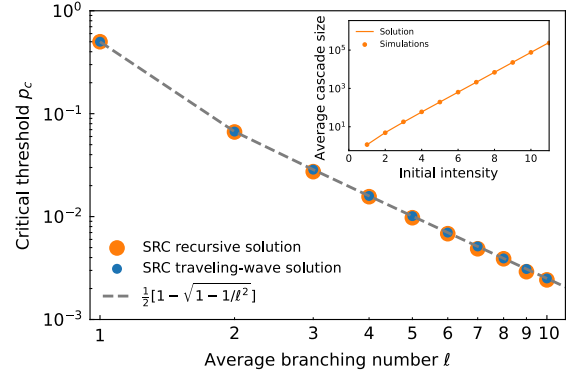

FIG. 3. Critical threshold p_c of SRC on Poisson trees of different average branching number ℓ. Results are obtained by solving the exact recursion in Eq. (1), the explicit solution in Eq. (4), and the critical condition of the traveling wave in Eq. (9). The results match up to the numerical precision at which we solve the recursion. The inset validates the explicit solution in Eq. (3) for the expected cascade size m_k, comparing it with 10^4 simulations per value of initial intensity, performed at $p = 0.01$ and $\ell = 3$.

$$m_k(p) = \frac{1}{\ell - 1}\left\{\left[\frac{1 - \sqrt{1 - 4p(1-p)\ell^2}}{2p\ell}\right]^k - 1\right\}. \quad (3)$$

We calculate the critical point p_c of the process as the value of p where the susceptibility of the system diverges, such that $dm_k/dp \to \infty$. We find

$$p_c = \frac{1}{2}\left(1 - \sqrt{1 - \ell^{-2}}\right). \quad (4)$$

Figure 3 validates the exact closed-form expressions above by comparing Eq. (4) against the solution from the exact recursion and Eq. (3) against numerical simulations (inset plot).

Temporal behavior—To get a better idea of the behavior of the system around the critical point, we analyze the depth of cascades and the associated temporal dynamics of intensity. We write a recursion for $Q_k(n)$, the cumulative probability that a cascade generated by a node of intensity k has depth not larger than n,

$$Q_k(n) = G[pQ_{k+1}(n-1) - (1-p)Q_{k-1}(n-1)], \quad (5)$$

with initial condition $Q_0(n) = 1 - \delta_{n,0}$. Crucially, solving for the tail $D_k(n) = 1 - Q_k(n)$ reveals that, independently of the initial intensity, the tail of the depth distribution decays exponentially for large n as $D(n) \sim \exp[-n\gamma_\ell(p)]$, with $\gamma_\ell(p) = -\ln\sqrt{4p(1-p)\ell^2}$. See SM for details [22].

At each generation n, we can calculate the expected maximal number of positive steps in intensity $P_{\max}(n, p)$ (i.e., the number of receptive nodes met) over all paths. To solve for the dynamics of $P_{\max}(n, p)$ we define the cumulative probability $R_n(x) = \text{Prob}[P_{\max}(n, p) \leq x]$, with

initial condition $R_0(x) = \mathbf{1}_{x \geq 0}$. This obeys the recursion

$$R_{n+1}(x) = G[pR_n(x-1) + (1-p)R_n(x)]. \quad (6)$$

We then use a traveling wave ansatz $R_n(x) = \tilde{R}(y = x - v_{\max}n)$. We linearize Eq. (6) in the region far ahead of the front and look for an exponential solution, $1 - \tilde{R}(y) \sim e^{-\mu y} \ll 1$. We find that the values of the velocity $v_{\max}$ and the decay exponent μ of the centered cumulative probability function $\tilde{R}(y)$ are related and found by solving a transcendental equation,

$$v_{\max}(p) = \frac{1}{\mu} \ln \left[\ell(1-p) + \ell p e^{\mu}\right] = \frac{p e^{\mu}}{1 - p + p e^{\mu}}. \quad (7)$$

The first equality comes from the linearization of Eq. (6); the second one from solving for the minimum value of the corresponding speed, in accordance to the principle of velocity selection [25].

The traveling wave ansatz comes with a universal logarithmic correction [26–28], such that we have $P_{\max}(n, p) = v_{\max}(p)n + (3/2\mu) \log n$. Assuming an initial intensity I_0, the expected maximal intensity $I_{\max}(n, p)$ after n generations will be I_0 plus the difference between positive and negative steps after n generation; that is,

$$\begin{aligned} I_{\max}(n, p) &= P_{\max}(n, p) - [n - P_{\max}(n, p)] + I_0 \\ &= 2P_{\max}(n, p) - n + I_0. \end{aligned} \quad (8)$$

By definition of p_c, $I_{\max}(n, p)$ should diverge as $n \to \infty$ for $p > p_c$ and go to zero for $p < p_c$. Therefore, at p_c,

$$\lim_{n\to\infty} \frac{dI_{\max}}{dn} = 2v_{\max}(p_c) - 1 = 0 \Rightarrow v_{\max}(p_c) = 1/2. \quad (9)$$

We again find p_c by imposing $v_{\max}(p_c) = 1/2$ in Eq. (7).

Extended critical behavior—Figure 4 shows that below p_c, the cascade size distributions of the SRC feature steep power-law tails with tunable scaling exponents $\tau > 2$. The exponent decreases when p increases until reaching $\tau = 2$ at $p = p_c$, as required for the expected cascade size to diverge. This behavior becomes even more persistent for more heterogeneous branching distributions [22].

Why do we find a critical-like scaling off the critical point? By combining all of our analyses, we can (i) estimate the scaling exponents in the subcritical regime, (ii) derive the critical exponent, and (iii) characterize the exponential cutoffs in the supercritical regime. Importantly, the presence of power-law tails in the subcritical regime has recently been proven in the context of killed branching random walks in Ref. [18] without explicit solutions for the scaling exponents.

Mathematically, cascade size increases exponentially with the intensity k as $s \sim \exp(ak)$, where a can be readily identified from Eq. (3). On the other hand, according to our traveling wave solution, the distribution of the maximal intensity $I_{\max}(n)$ at a given generation has an exponential tail. Based on the tail of cascade depth $D_k(n) = 1 - Q_k(n)$ from Eq. (5), we can integrate over exponentially decaying cascade depths. The tail of cascade sizes is then generated by the exponential of a quantity, $I_{\max}$, distributed with an exponential tail $e^{-bI_{\max}}$. This combination of exponentials is a known mechanism to produce power-law tails [30]. As detailed in SM [22], we can thus combine the rates a and b to estimate the scaling exponent
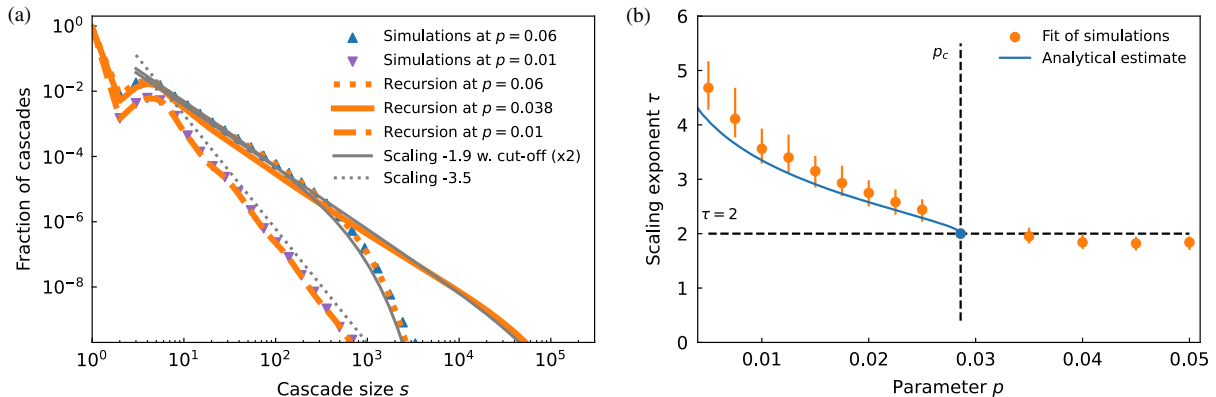

FIG. 4. Extended critical behavior around the critical point p_c for a Poisson tree of $\ell = 3 (p_c \approx 0.0286)$. (a) Cascade size distributions for p above and below p_c. Above p_c, we find a scaling relationship with exponential cutoff $s^{-\tau(p)} \times e^{-s/\bar{s}[n_c(p)]}$ based on the critical generation $n_c(p)$ given in Eq. (11) if p is close to p_c. Below p_c, we find arbitrarily steep power-law decays as a function of p; for instance, $\tau \approx 3.5$ for $p = 0.01$. Results from 10^8 simulations are reported for two p values with logarithmic binning. The recursion is exact. (b) Scaling exponents versus p obtained with our approximate solution, Eq. (10), and by fitting power-law tails to our exact solution from recursion. Goodness of fit is evaluated with the Kolmogorov-Smirnov (KS) statistic [29]; markers show its minima and lines show an acceptable range (KS < 0.05).
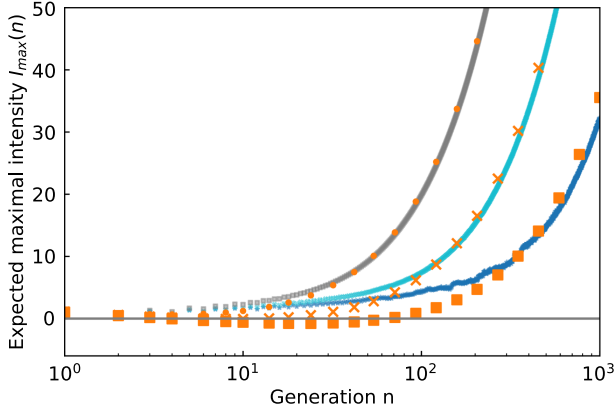
FIG. 5. Expected maximal intensity over generations n produced by the logarithmically corrected $I_{\max}(n, p)$ for different values $p > p_c$. We compare the solution with the average maximal intensity observed in at least 10^6 given the process is not extinct at generation $n - 1$. By definition, surviving cascades in simulations are always at intensity greater than zero. Nonetheless, the traveling wave solution captures the general long-time behavior of $I_{\max}(n, p)$.

$\tau(p) = 1 + b/a$ as

$$\tau(p) \approx 1 + \frac{\mu[1 - v_{\max}(p)] + \ln \sqrt{4p(1-p)\ell^2}}{\ln\left(1 - \sqrt{1 - 4p(1-p)\ell^2}\right) - \ln(2p\ell)} \quad (10)$$

when $p < p_c$, as shown in Fig. 4(b). Notice that, consistent with a derivation shown in our SM using only the traveling wave at $p = p_c$, Eq. (10) correctly predicts $\tau(p_c) = 2$.

Moving to the supercritical regime, we can characterize the distributions further using the universal logarithmic correction to $P_{\max}(n, p)$. This correction implies that the process is expected to spend $n_c(p)$ generations close to extinction before the linear growth of the wave front dominates (validated in Fig. 5). At small n, the critical condition reads $dI_{\max}/dn = 2v_{\max}(p) - 1 - 3/(\mu n) = 0$, and we find

$$n_c(p) = \frac{3}{\mu[2v_{\max}(p) - 1]}. \quad (11)$$

As is the case with most cascade models, we expect an exponential cutoff on the cascade size distribution which is here imposed by the critical generation n_c and should thus be of order $\bar{s}(n_c) = (\ell^{n_c} - 1)/(\ell - 1)$, the maximum size a cascade can reach by generation n_c. We estimate the cascade size s to be distributed as a power law with exponential cutoff $s^{-\tau(p)} \times e^{-s/\bar{s}(n_c(p))}$. As Fig. 4(a) shows for $p = 0.038$, for which $n_c \approx 10.66$ and $\tau \approx 1.9$, our estimation is in excellent agreement with the exact results from recursion. Nonetheless, as the value of p

increases, n_c decreases, and additional correction terms would eventually come into play to push the cutoff to higher values (first with a nonuniversal term of order $1/\sqrt{n}$) [28]. We illustrate this using $p = 0.06$ in Fig. 4(a), where Eq. (11) predicts $n_c \approx 3.91$, yet we obtain a much better fit with the value $n_c = 6$ used in the figure. However, the exact value of $\tau(p > p_c)$, and whether this value truly deviates from $\tau(p_c) = 2$, remains an open problem.

Discussion—The self-reinforcing cascade process is a parsimonious model to capture the fact that the strength of individual beliefs or the quality of products may vary and thus influence their ability to spread further. This variability is aligned with real-world phenomena, where not all individuals or contents are equally influential in the transmission of ideas or behaviors. With this simple mechanism, the SRC model can produce a wide range of scaling behaviors for cascade size distributions, whereas classic cascade models are constrained by a unique and universal scaling exponent obtained only at a precise critical point.

The shape and statistics of SRC are surprising in two ways. One, they follow a fat-tailed cascade size distribution in their subcritical regime. Two, the tail of their depth distribution remains exponential even at the critical point. Thus, subcritical and critical SRC are short but very broad compared to classic cascade models. The unique shape of SRC could help identify signatures of varying cascade intensity or quality in empirical data. We could expect this mechanism to appear in cascades where content is able to change (e.g., mutations in epidemics or personalized social media posts) as opposed to cascade with fixed content (e.g., cascade of clones, or reposting in social media), and SRC could provide more realistic models in these cases. In addition, the search remains open for a general model that provides anomalous exponents for both size and depth distributions as found empirically [1].

We outlined several important properties of self-reinforcing cascades and proposed a few analytical approaches to better understand these processes: exact probability generating functions for cascade size, exact recursions over cascade depth, and the traveling wave technique for cascade intensity. Combining all three approaches, we were able to characterize the different scaling behaviors produced by the model. Altogether, this effort may provide a useful framework for those seeking to understand cascading behavior in complex real-world systems.

Data availability—The data that support the findings of this Letter are openly available [31].

———————

[1] Daniele Notarmuzi, Claudio Castellano, Alessandro Flammini, Dario Mazzilli, and Filippo Radicchi, Universality, criticality and complexity of information propagation in social media, Nat. Commun. **13**, 1308 (2022).

[2] Theodore Edward Harris *et al.*, *The Theory of Branching Processes* (Springer, Berlin, 1963), Vol. 6.

[3] Filippo Radicchi, Claudio Castellano, Alessandro Flammini, Miguel A. Muñoz, and Daniele Notarmuzi, Classes of critical avalanche dynamics in complex networks, Phys. Rev. Res. **2**, 033171 (2020).

[4] Márton Karsai, Kimmo Kaski, Albert-László Barabási, and János Kertész, Universal features of correlated bursty behaviour, Sci. Rep. **2**, 397 (2012).

[5] Ryosuke Nishi, Taro Takaguchi, Keigo Oka, Takanori Maehara, Masashi Toyoda, Ken-ichi Kawarabayashi, and Naoki Masuda, Reply trees in twitter: Data analysis and branching process models, Social Network Anal. Mining **6**, 1 (2016).

[6] Karol Wegrzycki, Piotr Sankowski, Andrzej Pacuk, and Piotr Wygocki, Why do cascade sizes follow a power-law?, in *Proceedings of the 26th International Conference on World Wide Web* (2017), pp. 569–576.

[7] Javier Borge-Holthoefer, Alejandro Rivero, Iñigo García, Elisa Cauhé, Alfredo Ferrer, Darío Ferrer, David Francos, David Iniguez, María Pilar Pérez, Gonzalo Ruiz *et al.*, Structural and dynamical patterns on online social networks: The Spanish May 15th Movement as a case study, PLoS One **6**, e23883 (2011).

[8] Filippo Zimmaro and Henrik Olsson, A meta-model of belief dynamics with personal, expressed and social beliefs, arXiv:2502.14362.

[9] Mirta Galesic, Henrik Olsson, Jonas Dalege, Tamara Van Der Does, and Daniel L. Stein, Integrating social and cognitive aspects of belief dynamics: Towards a unifying framework, J. R. Soc. Interface **18**, 20200857 (2021).

[10] Linus Nyman, Understanding Code Forking in Open Source Software: An Examination of Code Forking, *Its Effect on Open Source Software, and How it is Viewed and Practiced by Developers* (Hanken School of Economics, Helsinki, Finland, 2015).

[11] Robert Viseur, Forks impacts and motivations in free and open source projects, Int. J. Adv. Comput. Sci. Appl. **3**, 117 (2012).

[12] Jonas Gamalielsson and Björn Lundell, Sustainability of open source software communities beyond a fork: How and why has the LibreOffice project evolved?, J. Syst. Software **89**, 128 (2014).

[13] Jailton Coelho and Marco Tulio Valente, Why modern open source projects fail, in *Proceedings of the 2017 11th Joint Meeting on Foundations of Software Engineering* (2017), pp. 186–196.

[14] S. Redner, L. Hébert-Dufresne, and P. L. Krapivsky, Long-range fire propagation (to be published).

[15] Daniele Notarmuzi, Claudio Castellano, Alessandro Flammini, Dario Mazzilli, and Filippo Radicchi, Percolation theory of self-exciting temporal processes, Phys. Rev. E **103**, L020302 (2021).

[16] James P. Gleeson, Jonathan A. Ward, Kevin P. O'Sullivan, and William T. Lee, Competition-induced criticality in a model of meme popularity, Phys. Rev. Lett. **112**, 048701 (2014).

[17] Harry Kesten, Branching Brownian motion with absorption, Stoch. Proc. Appl. **7**, 9 (1978).

[18] E. F. Aidékon, Y. Hu, and O. Zindy, The precise tail behavior of the total progeny of a killed branching random walk, Ann. Probab. **41**, 3786 (2013).

[19] Herbert S. Wilf, *Generating Functionology* (Academic Press, New York, 1994).

[20] James P. Gleeson, Tomokatsu Onaga, Peter Fennell, James Cotter, Raymond Burke, and David J. P. O'Sullivan, Branching process descriptions of information cascades on Twitter, J. Complex Netw. **8**, cnab002 (2020).

[21] M. E. J. Newman, S. H. Strogatz, and D. J. Watts, Random graphs with arbitrary degree distributions and their applications, Phys. Rev. E **64**, 026118 (2001).

[22] See Supplemental Material at http://link.aps.org/supplemental/10.1103/5mph-sws5 for additional analyses.

[23] See notebook at http://bit.ly/SRCnotebook to reproduce the calculations.

[24] Michael Molloy and Bruce Reed, A critical point for random graphs with a given degree sequence, Random Struct. Algorithms **6**, 161 (1995).

[25] Satya N. Majumdar and P. L. Krapivsky, Extremal paths on a random Cayley tree, Phys. Rev. E **62**, 7735 (2000).

[26] Maury D. Bramson, Maximal displacement of branching Brownian motion, Commun. Pure Appl. Math. **31**, 531 (1978).

[27] Éric Brunet and Bernard Derrida, Shift in the velocity of a front due to a cutoff, Phys. Rev. E **56**, 2597 (1997).

[28] Éric Brunet, Some aspects of the Fisher-KPP equation and the branching Brownian motion, Habilitation à diriger des recherches, UPMC, 2016, https://theses.hal.science/tel-01417420.

[29] Aaron Clauset, Cosma Rohilla Shalizi, and Mark E. J. Newman, Power-law distributions in empirical data, SIAM Rev. **51**, 661 (2009).

[30] M. E. J. Newman, Power laws, Pareto distributions and Zipf's law, Contemp. Phys. **46**, 323 (2005).

[31] L. Hébert-Dufresne, Self-reinforcing cascades notebook (2025), https://bit.ly/SRCnotebook.